Received: 4 June 2021 | Revised: 8 August 2021 | Accepted: 16 August 2021

DOI: 10.1096/fj.202100929R

THE FASEB JOURNAL

RESEARCH ARTICLE

The fasting-feeding metabolic transition regulates mitochondrial dynamics

Mauricio Castro-Sepúlveda[1,2] | **Béatrice Morio**[3] | **Mauro Tuñón-Suárez**[1] | **Sebastian Jannas-Vela**[1] | **Francisco Díaz-Castro**[4,5] | **Jennifer Rieusset**[3] | **Hermann Zbinden-Foncea**[1,6]

[1]Laboratorio de Ciencias del Ejercicio, Escuela de Kinesiologia, Facultad de Medicina, Universidad Finis Terrae, Santiago, Chile

[2]Facultad de Medicina, Pontificia Universidad Católica de Chile, Santiago, Chile

[3]CarMeN Laboratory, UMR INSERM U1060/INRA U13397, Université Claude Bernard Lyon 1, Pierre-Bénite, France

[4]Laboratorio de Investigación en Nutrición y Actividad Física (LABINAF), Instituto de Nutrición y Tecnología de los Alimentos, Universidad de Chile, Santiago, Chile

[5]Laboratorio de Autofagia y Metabolismo, Departamento de Fisiología, Facultad de Ciencias Biológicas, Pontificia Universidad Católica de Chile, Santiago, Chile

[6]Centro de Salud Deportiva, Clínica Santa María, Santiago, Chile

Correspondence
Mauricio Castro-Sepúlveda and Hermann Zbinden-Foncea, Laboratorio de Ciencias del Ejercicio, Facultad de Medicina, Universidad Finis Terrae, Santiago, Chile. Av. Pedro de Valdivia 1509, Providencia, Chile.
Email: mcastro@uft.cl (M. C.-S.) and hzbinden@uft.cl (H. Z.-F.)

Funding information
This study was funded by Research Grant awarded to MCS by Universidad

Abstract

In humans, insulin resistance has been linked to an impaired metabolic transition from fasting to feeding (metabolic flexibility; MetFlex). Previous studies suggest that mitochondrial dynamics response is a putative determinant of MetFlex; however, this has not been studied in humans. Thus, the aim of this study was to investigate the mitochondrial dynamics response in the metabolic transition from fasting to feeding in human peripheral blood mononuclear cells (PBMCs). Six male subjects fasted for 16 h (fasting), immediately after which they consumed a 75-g oral glucose load (glucose). In both fasting and glucose conditions, blood samples were taken to obtain PBMCs. Mitochondrial dynamics were assessed by electron microscopy images. We exposed in vitro acetoacetate-treated PBMCs to the specific IP3R inhibitor Xestospongin B (XeB) to reduce IP3R-mediated mitochondrial Ca^{2+} accumulation. This allowed us to evaluate the role of ER-mitochondria Ca^{2+} exchange in the mitochondrial dynamic response to substrate availability. To determine whether PBMCs could be used in obesity context (low MetFlex), we measured mitochondrial dynamics in mouse spleen-derived lymphocytes from WT and ob/ob mice. We demonstrated that the transition from fasting to feeding reduces mitochondria-ER interactions, induces mitochondrial fission and reduces mitochondrial cristae density in human PBMCs. In addition, we demonstrated that IP3R activity is key in the mitochondrial dynamics response when PBMCs are treated with a fasting-substrate in vitro. In murine mononuclear-cells, we confirmed that mitochondria-ER interactions are regulated in the fasted-fed transition and we further highlight mitochondria-ER miscommunication in PBMCs of diabetic mice. In conclusion, our results demonstrate that the fasting/feeding transition reduces mitochondria-ER interactions, induces mitochondrial fission and reduces mitochondrial cristae density in human PBMCs, and that IP3R activity may potentially play a central role.

Abbreviations: AcAc, acetoacetate; ER, endoplasmic reticulum; MetFlex, metabolic flexibility; MNCs, spleen-derived mononuclear cells; NEFA, non-esterified fatty acid; OCR, oxygen consumption rate; PBMCs, peripheral blood mononuclear cells; PLA, proximity ligation assays; RQ, respiratory quotient; XeB, Xestospongin B.

Finis Terrae (Grant no. CAI 2019). The work was further supported by Universidad Finis Terrae through projects grants awarded to HZF

KEYWORDS

fasting, mitochondria-ER interaction, mitochondrial cristae, mitochondrial fusion, mitochondrial morphology, obesity

1 | INTRODUCTION

Metabolic flexibility (MetFlex) is the capacity of an organism, an organ, or a single cell to adapt fuel oxidation to fuel availability, as exemplified by the metabolic transition from fasting to feeding.[1] In humans, impaired MetFlex to glucose and lipid availability has been associated with insulin resistance,[2] and weight gain,[3] which is characteristic of obese and type 2 diabetic patients. Recently, a direct relationship between MetFlex measured during a glucose clamp and in response to a long fast (ketone bodies) was observed.[4] This suggests that the cellular mechanisms that regulate MetFlex to different substrates may have a common and dynamic (on/off) mechanism. However, to date, this mechanism remains to be fully elucidated.

Mitochondria are intracellular organelles that sense nutrients and adapt the cellular metabolism to nutrient availability[5] through changes in mitochondrial dynamics, including (i) mitochondrial network (mitochondrial fusion and fission), (ii) mitochondrial inter-organellar interactions, such as with the endoplasmic reticulum (mitochondria-ER) and (iii) intra-mitochondrial dynamics to shape cristae and adjust matrix volume.[6] Recent evidence suggest that mitochondrial dynamics response is involved in MetFlex.[7] For example, rodents who underwent an overnight fast and are predominantly oxidising lipids, have hepatic mitochondria that exhibit a fusion phenotype—larger mitochondria—with a concomitant increase in mitochondria-ER interactions. However, after feeding when glucose availability and oxidation predominate, mitochondria exhibit a fission phenotype—smaller mitochondria—and reduced ER-interaction.[8] In agreement, we recently observed that relative whole-body fatty acid oxidation was directly associated with a mitochondrial fusion phenotype and an increased mitochondria-sarcoplasmic reticulum interaction in human skeletal muscle.[9] This suggests that similar mitochondrial responses occur in both mice and humans as well as in liver and skeletal muscle tissue. Another aspect of mitochondrial dynamics is mitochondrial cristae. Recently, advanced super-resolution techniques revealed that cristae are highly dynamic independent bioenergetic units that can remodel on a timescale of seconds (like intra-mitochondrial dynamics).[10] Interestingly, it appears that the hepatic metabolic shift relies on the parallel remodeling of mitochondrial cristae and mitochondria-ER interactions, which probably is mediated by Ca^{2+} signaling.[11,12] As such, cristae width and density were recently demonstrated to be affected by glucose in cell cultures.[13,14] Altogether, these results suggest that the mitochondrial dynamics response (including dynamic regulations of mitochondria-ER interactions, mitochondrial network and mitochondrial cristae) are putative determinants of MetFlex. However, whether these dynamic responses occur concomitantly when substrate availability is modified in humans has not been studied.

Recently, human metabolic studies have used peripheral blood mononuclear cells (PBMCs)[15,16] because, unlike other tissues, blood can be obtained in a minimally-invasive manner from healthy individuals and is a potential physiological cellular marker of the whole-body status. Furthermore, mitochondrial PBMCs metabolism reflects nutrition-related metabolic changes, such as fasting.[17,18] Therefore, PBMCs represent an ideal minimally-invasive cellular model to elucidate mitochondrial dynamics responses to substrate availability in humans.

Thus, the purpose of this study was to investigate the mitochondrial dynamics responses in the metabolic transition from fasting to feeding in human PBMCs. We hypothesized and demonstrated that the switch from fatty acid oxidation to enhanced glucose oxidation (as observed during fasting/feeding transition) reduces mitochondria-ER interactions, induces mitochondrial fission and reduces mitochondrial cristae density. In addition, we demonstrated that IP3R activity (regulator of ER-mitochondria calcium $[Ca^{2+}]$ exchange) is key in the mitochondrial dynamics responses when PBMCs are treated in vitro with a fasting-substrate. In murine spleen-derived mononuclear cells (MNCs), we confirmed the regulation of mitochondria-ER interactions during fed-fasted transition and we further highlighted mitochondria-ER miscommunication in MNCs of obese and diabetic mice. Our study suggests a potential role of the mitochondrial dynamics responses on MetFlex in humans, in which IP3R plays a central role. Besides, this study highlights the use of PBMCs to investigate the nutritional regulation of mitochondrial dynamics in clinical intervention studies to identify preventive or therapeutic strategies to reverse low MetFlex in obese and type 2 diabetic patients.

2 | MATERIALS AND METHODS

2.1 | Human trials

Participants (n = 6 healthy males; 32.5 [8.0] years, 23.4 [1.6] kg/m^2), with no history of cardiovascular,

respiratory, or thyroid disease, were included in the study. Subjects signed a written informed consent form prior to study participation and were instructed to avoid vigorous physical activity on the day prior to metabolic testing, and to maintain their usual dietary habits. On the day of testing, subjects visited the laboratory after a ~ 16-h fast and rested for 30 min in a supine position, under thermoneutral conditions. Gas exchange was measured in the fasted state for 15 min using a breath-by-breath pulmonary gas exchange analyzer system (Ergocard, Medisoft, Belgium). Immediately after, participants consumed a 75-g oral glucose load, and 45 min later, gas exchange was measured for 30 min at rest. After gas exchange analysis of both fed and fasted conditions, blood samples (10 ml) were collected from the antecubital vein to isolate PBMCs and analyze blood metabolites. The protocol was approved by Finis Terrae University Ethical Board and adhered to the Declaration of Helsinki.

2.2 | Gas exchange

The gas analyzer was calibrated prior to each measurement using gases of known concentrations (O_2 = 16% and CO_2 = 4%). The airflow was calibrated using a 3-liter syringe (Hans Rudolph, United States). Respiratory quotient (RQ; CO_2 produced/O_2 consumed) was used as a marker of whole-body relative substrate oxidation, with lower values indicating higher fatty acid than glucose oxidation. To estimate RQ, subjects lay in a supine position for 30 min wearing the gas analyzer mask. The average of the final five minutes was used for analysis.[9]

2.3 | Blood analysis

Blood serum was used to determine glucose (Freestyle Optium Neo, Abbott, Chile), ß-hydroxybutyrate (Freestyle Optium Neo, Abbott, Chile), lactate (Lactate Pro 2™, KDK, Japan) and non-esterified fatty acid (NEFA; NEFA-HR, Wako Diagnostics, Richmond, VA, USA) concentrations.

2.4 | PBMC isolation

From ~10 ml of freshly drawn blood, PBMCs were separated under sterile conditions on Ficoll-Histopaque 1077 (Sigma, Milan, Italy) gradients using the method described by Belia et al (1976), to obtain ~80% lymphocytes. Aliquots of heparinized whole blood diluted with an equal volume of Dulbecco's phosphate buffered saline were gently applied to an equal volume of Ficoll-Histopaque 1077 in centrifuge tubes.[19,20] Samples were centrifuged at 1500 rpm for 50 min, and the resultant interface was carefully aspirated from the gradient and washed 3 times in Dulbecco's PBS.[19,20] PBMCs were divided into three aliquots: (1) frozen in liquid nitrogen and stored at −80°C for western blotting; (2) fixed in 2.5% glutaraldehyde for transmission electron microscopy analyses and; (3) resuspended in PBS to determine cell O_2 consumption.

2.5 | Western Blotting

PBMCs were homogenized in a lysis buffer containing: 20 mM Tris-HCl (pH 7.5), 1% Triton X-100, 2 mM EDTA, 20 mM NaF, 1 mM Na2P2O7, 10% glycerol, 150 mM NaCl, 10 mM Na3VO4, 1 mM PMSF, and a protease inhibitor cocktail (Complete TM, Roche Applied Science). Proteins were separated by SDS-PAGE, and transferred to PVDF membranes, as described previously.[9] The following antibodies and dilutions were used: Mfn2 (1:1000; cat. no. ab56889, Abcam), Opa1 (1:1000; cat. no. 612606, BD Biosciences), Phospho-Drp1 (Ser616) (1:1000; cat. no. 3455, Cell Signaling), Fis1 (1:1000; cat. no. ALX-210-1037, Enzo Life Sciences), total *OXPHOS* cocktail (1:1000; cat. no. ab110413, Abcam), Mic60 (1:1000; cat. no. 10179-1-AP, Proteintech) and Mic19 (1:1000; cat. no. 25625-1-AP, Proteintech). Ponceau was used as loading control. Image acquisition and band quantification were performed using the ChemiDoc™ MP System and Image Lab 5.0 software (Bio- Rad).

2.6 | Electron microscopy

Fixed PBMCs were dissected, washed four times with 0.1 M sodium cacodylate buffer, and stained with 2% osmium tetroxide in 0.1 M sodium cacodylate buffer for 2 h. Samples were then washed with water and stained with 1% uranyl acetate for 2 h. Subsequently, the samples were dehydrated using an acetone dilution series and embedded in Epon. Lastly, 80-nm sections were cut, mounted on electron microscopy grids, and examined using a transmission electron microscope (Philips, Tecnai 12 at 80 kV). Morphometric analyses of PBMCs were performed on longitudinal sections using Fiji/ImageJ software.[9,21] For the generic characterization of the morphology and abundance of mitochondria, a mask was drawn over the largest possible cytosolic area. The percentage of the cytosolic area covered by mitochondria was used as the 2D equivalent of mitochondrial density [9]. Mitochondria density and size were assessed in 4-6 individual cells per subject at 20500x magnification. The mitochondrial size (μm^2) was calculated as the mean area of each organelle in the cell. The mitochondria-ER interactions were assessed at

43 000 × magnification and analyzed when both organelles were <50 nm apart from the outer mitochondrial membrane.[9,21] The gap distance for each interaction was averaged using three individual distance readings evenly distributed over the interface length.[9,21] Mitochondrial cristae were assessed at 43 000 × magnification and were identified manually as described previously.[11]

2.7 | O_2 consumption

Live PBMCs were resuspended (10^6 cells/500 ml) in DMEM without glucose and placed in gas-tight chamber. Cell number and viability were assessed using BioRad's Automated Cell Counter TC20. Basal oxygen consumption rate (OCR) was measured at 37°C using a Clark electrode (Yellow Springs Instruments) for three minutes.

2.8 | Cell culture experiments

After obtaining written informed consent, another set of healthy subjects, (different from the participants of the in vivo study; $n = 3$ healthy males; 31.4 [3.0] years, 23.8 [2.4] kg/m^2) donated 10 ml of blood after an overnight fast, from which PBMC were isolated. The cells of the three donors were pooled and divided into three conditions for four hours; (1) Glucose; DMEM (does not contain glucose, pyruvate, and glutamine [Invitrogen]) supplemented with 10% dialyzed FBS, 10 mM glucose, and penicillin/streptomycin. (2) Acetoacetate (AcAc); DMEM does not contain glucose, supplemented with 10% dialyzed FBS, 10 mM AcAc, and penicillin/streptomycin. (3) AcAc + XeB; DMEM does not contain glucose, supplemented with 10% dialyzed FBS, 10 mM AcAc, XeB (XeB; 1 μM) and penicillin/streptomycin. After four hours of stimulation, the PBMCs were washed three times in PBS and immediately divided into two aliquots: (1) fixed in 2.5% glutaraldehyde for transmission electron microscopy analyses and (2) resuspended for measurement O_2 consumption. Three independent experiments were performed.

2.9 | Murine spleen-derived mononuclear cells isolation

MNCs were isolated from the spleen of overnight fasted and fed wild-type and ob/ob male mice, previously used for the analysis of hepatic ER-mitochondria interactions.[8] The metabolic characteristics of these mice was previously reported.[8] Spleens were transported on ice in RPMI 1640 medium containing 200 U/ml penicillin, 200 μg/ml streptomycin, 100 μg/ml gentamicin and 10% fetal calf serum (RPMI+). Spleens were placed on a sterile petri dishes and gently infused with culture medium using a syringe. The spleen suspension was filtered at 40 μm and then centrifuged for 10 min at 1800 rpm. Cells were incubated with 10 ml NH_4Cl 1x for 10 min at RT, 10 ml RPMI+ was added and the suspension was centrifuged for 10 min at 1800 rpm. Spleen-derived MNCs were counted and frozen in fetal calf serum containing with 10% DMSO. After thawing, cells were suspended in RPMI+ and cultured in 35 mm glass bottom culture dishes (MatTek Corporation, Ashland, USA) for 24 h.

2.10 | In situ proximity ligation assay

Spleen-derived MNCs were gently washed, fixed with 10% formaldehyde, washed with 1x PBS and permeabilized with 0.1% triton. MNCs were then incubated overnight at 4°C with a binary primary antibody mixture of anti-IP3R (H-80, Santa Cruz Biotechnology, Dallas, USA) and VDAC1 (ab14734, Abcam, Cambridge, UK). After two washes with 0.05% TBS-Tween, cells were incubated for 1 h at 37°C with the complementary secondary antibody (Rabbit PLUS and Mouse MINUS). Proximity ligations were performed according to the manufacturer's protocols (Sigma Aldricht, Saint-Quentin Fallavier, France). Lymphocytes were tagged using FITC-labelled anti-IgA (1/60 dilution, ab9161, Abcam, Cambridge, UK). Preparations were mounted in Duolink II mounting medium containing DAPI. Fluorescence was analyzed with a Zeiss inverted fluorescent microscope using the AxioVision program (z-stack imaging, microscopy magnification x160). Fluorescent dot signals were quantified using BlobFinder Software (v3.2, Center for Image Analysis, Uppsala University). Results were expressed as number of blobs per nucleus. A minimum of 30 images were taken per sample, and five independent series were performed for each treatment.

2.11 | Statistics

Data are presented as mean [standard deviation]. Blood markers, RQ, OCR, mitochondria-ER interactions, mitochondrial morphology markers and western blot after 16 h-fasting versus 45 min-after glucose consumption were compared using a paired t-test. The in vitro conditions and murine experiments were compared with one-way ANOVA with a Tukey's post-test. $p < .05$ was considered as statistically significant. Prism 7 (GraphPad Software, La Jolla, CA, USA) was used for analyses.

3 | RESULTS

3.1 | Human trial, mitochondria-ER, and MetFlex in human PBMCs

As expected, the RQ during fasting was lower than after the glucose load (0.75 ± 0.05 to 0.84 ± 0.06 mmol/L; $p = .034$; Figure 1C). In addition, blood glucose (97.2 ± 5.4 to 171 ± 24.1 mg/dl; $p = .031$; Figure 1A) and lactate concentrations (1.3 ± 0.4 to 2.3 ± 1.1 mmol/L; $p = .030$; Figure 1B) were lower in the fasted condition than the glucose condition, whilst NEFA (0.42 ± 0.27 to 0.03 ± 0.03 mmol/L; $p = .049$; Figure 1D) and ß-hydroxybutyrate (0.22 ± 0.13 to 0.02 ± 0.04 mM; $p = .031$; Figure 1E) concentrations were higher.

3.2 | Mitochondrial dynamics, OXPHOS activity, and MetFlex in human PBMCs

As substrate availability and oxidation differed between these two conditions, we investigated whether the interactions between ER and mitochondria in PBMCs would respond to changes in substrate availability. We observed that the glucose condition was associated with increased mitochondria-ER distance and decreased mitochondria-ER interactions compared to the fasted condition (Figure 2A–C; $p = .003$ and $p = .007$). Furthermore, our results showed that the switch from fatty acids to glucose oxidation reduced OCR (*OXPHOS* activity; Figure 2D; $p = .03$) and induced a mitochondrial fragmentation phenotype (Figure 2F–H; $p < .05$), without changing mitochondrial density (Figure 2E; $p < .05$). Furthermore, glucose ingestion decreased Mfn2 protein (Figure 3A,B; $p = .03$), but did not affect OPA1, Fis1 or pDRP1^{Ser616} protein levels (Figure 3A,C–E). Similarly, glucose ingestion specifically decreased Mfn2 protein when mitochondrial fusion and fission proteins were adjusted to CIV-MTCO1 protein (Figure S1). We also observed reduced expression of CV-ATP5A (Figure 3F–G; $p = .063$), but no changes in other mitochondrial complexes protein expression (Figure 3F,H–J).

3.3 | Mitochondria cristae remodelling and MetFlex in human PBMCs

Compared to the fasted condition, the glucose condition reduced the mitochondrial cristae alignment, mitochondrial cristae number, and the total length of mitochondrial cristae (Figure 4A–E; $p = .007$, $p = .03$, $p = .002$, respectively), without affecting the expression of MIC19 and MiC60 proteins (Figure 4F–H) that form part of the MICOS complex. Similar results were observed when the expression of MIC19 and MiC60 proteins was adjusted to CIV-MTCO1 protein (Figure S2).

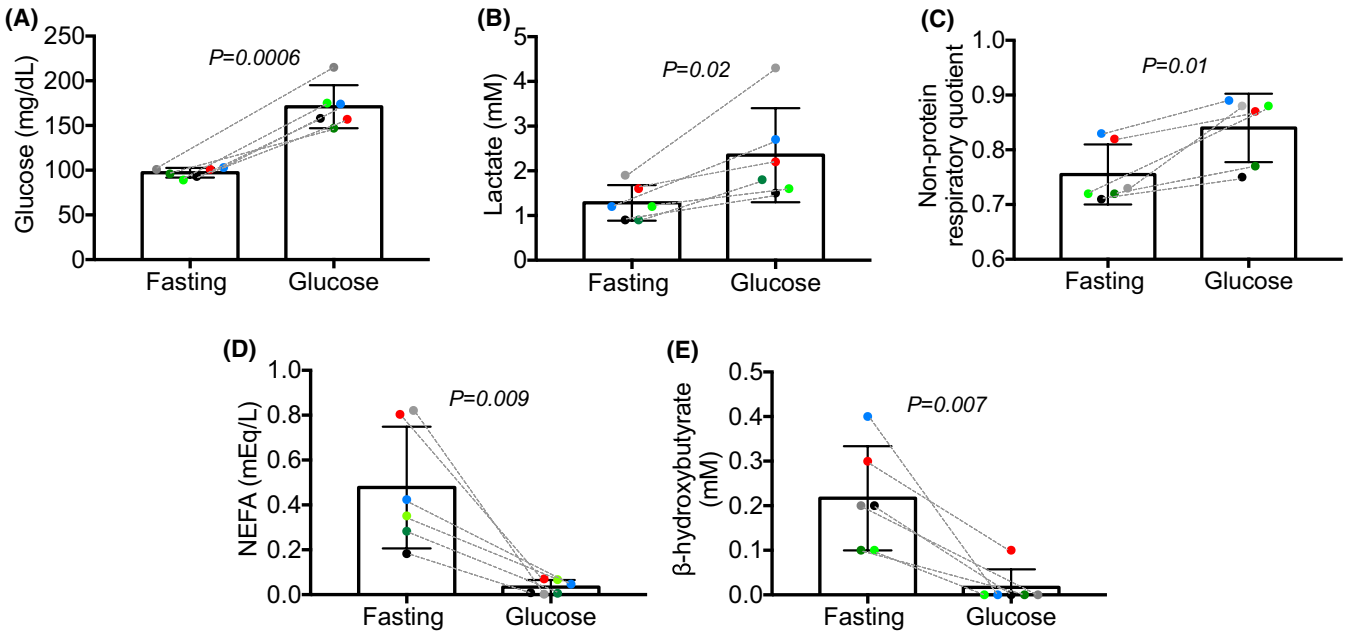

FIGURE 1 Blood analyses and non-protein respiratory quotient after fasting and after glucose load. Circulating concentrations of glucose (A), lactate (B), nonesterified fatty acid (NEFA) (D), β-hydroxybutyrate (E) and non-protein respiratory quotient (C) after fasting and after glucose load. In the graphs, each individual colored point represents an individual subject

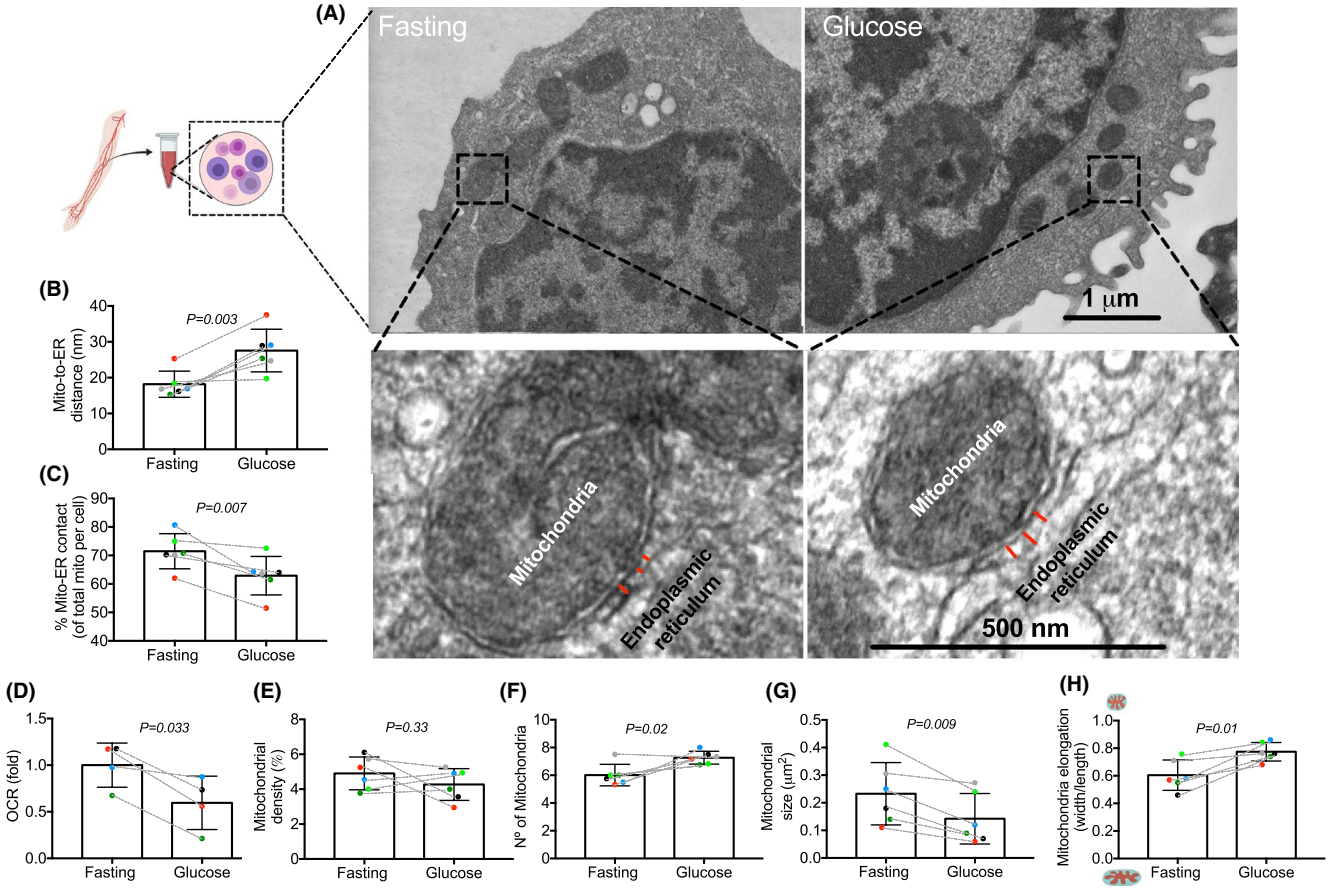

FIGURE 2 Mitochondria-ER interaction and mitochondrial morphology after fasting and after glucose load in human PBMCs. Representative transmission electron microscopy of mitochondria-ER interactions in human PBMCs after fasting and after glucose load (A). Quantification of mitochondria-ER distance (<50 nanometers) (B) and percentage of mitochondria-ER interactions (<50 nanometers) (C). Basal oxygen composition rate of PBMCs after fasting and glucose load $n = 4$ (D). Effects of fasting and glucose load on mitochondrial density (E). Effects of fasting and glucose load on mitochondria number (F), mitochondrial size (G) and mitochondria network (H). $n = 6$ healthy males, 4-6 cells per subject, >5 mitochondria per cell. Red lines indicate the distance between mitochondria and ER. In the graphs, each individual colored point represents an individual subject

3.4 | In vitro mitochondria-ER interaction and MetFlex

Previous studies suggest that changes in mitochondrial dynamics as a result of changes in substrate availability is regulated by IP3R-mediated mitochondrial Ca^{2+} accumulation. This hypothesis was included in our proposed model (Figure 5) and was tested in vitro. To evaluate the potential role of the ER-mitochondria Ca^{2+} exchange in the mitochondrial dynamic response to substrate availability, we used XeB, a specific IP3R inhibitor, which reduces IP3R-mediated mitochondrial Ca^{2+} accumulation. In vitro, reproducible differences in *OXPHOS* activity, mitochondria-ER distance, mitochondrial morphology and -cristae between the fasted state and the oral glucose load were obtained in PBMCs treated with AcAc (a fasting-substrate) or glucose (Figure 5A–E). XeB inhibited the effects of AcAc on the mitochondrial dynamics response (Figure 5A–E).

3.5 | Mitochondria-ER interactions, MetFlex, and obesity in murine spleen-derived lymphocytes

To determine whether mononuclear cells could be used in a pathological context to follow mitochondria-ER interactions (key in mitochondrial dynamic response), we switched on obese mice (low MetFlex) spleen-derived lymphocytes. MNCs were isolated from the spleens of wt and *ob/ob* mice, in both overnight fasted and fed states (Figure 6A). Mitochondria-ER interactions were measured by in situ proximity ligation assays (PLA). As shown in Figure 6, the switch from fasted to fed state is associated with a significant reduction of VDAC1-IP3R proximity. Interestingly, mitochondria-ER proximity is less in MNCs of fasted ob/ob mice than fasted wild-type mice (Figure 6A,B, $p < .05$); and did not decrease the interaction of organelles by the nutritional transition from the fasting state to the fed state in *ob/ob* MNCs (Figure 6B).

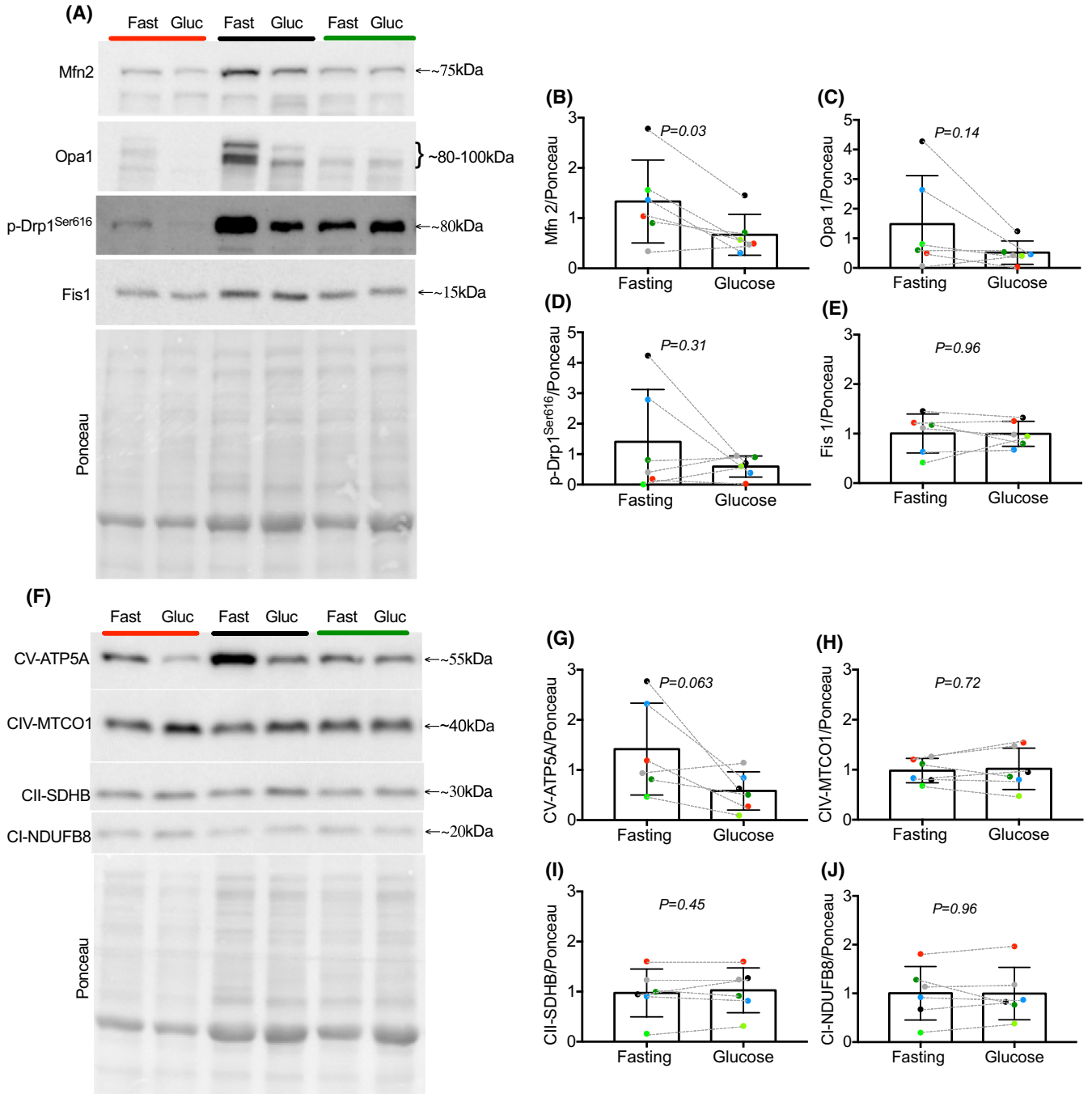

FIGURE 3 Mitochondrial fusion and fission and *OXPHOS* proteins after fasting and after glucose load in human PBMCs. Representative images of western blots (3 subjects) for the protein expression of mitochondrial fusion and fission (A), *OXPHOS* complexes proteins (F) and Ponceau in human PBMCs. Effects of fasting and glucose load on Mfn 2 (B), Opa 1 (C), p-Drp1^{Ser616} (D), Fis 1 (E) and *OXPHOS* complexes proteins (G-J). $n = 6$ healthy males. In the graphs, each individual colored point represents an individual subject. Glu, Glucose; Fast, Fasting

4 | DISCUSSION

Here, we investigated the mitochondrial dynamics responses in the metabolic transition from fasting to feeding and showed that this dynamic switch is associated with reduced mitochondria-ER interactions, increased mitochondrial fragmentation, and decreased mitochondrial cristae density in human PBMCs. In addition, we demonstrated that IP3R activity is key in the mitochondrial dynamics response when PBMCs are treated in vitro with a fasting-substrate. Lastly, we confirmed the regulation of mitochondria-ER interactions during the transition from fasting to feeding in murine wild-type spleen-derived MNCs, and further highlighted that alterations of

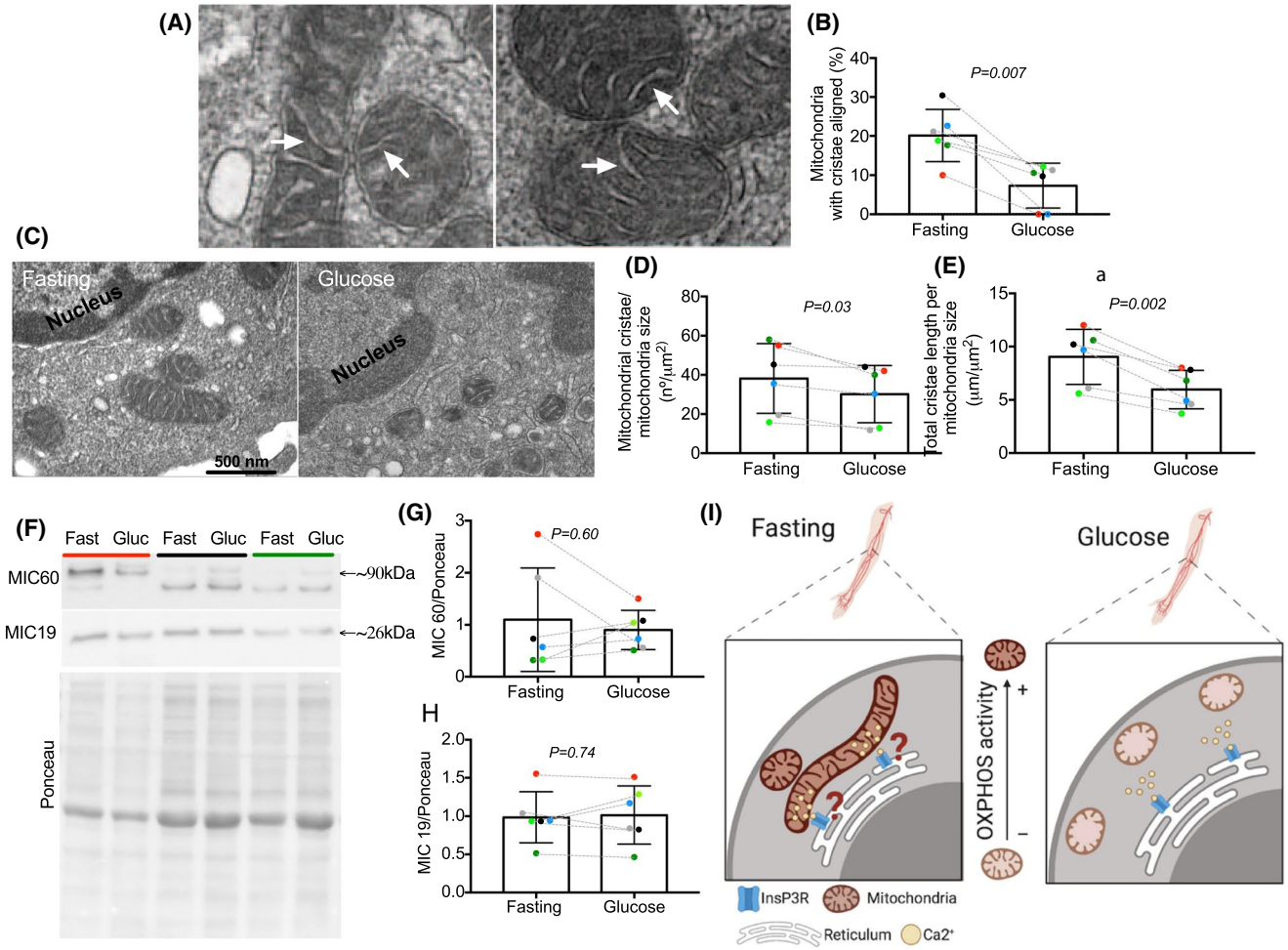

FIGURE 4 Intramitochondrial interaction and cristae density after fasting and after glucose load in human PBMCs. Representative transmission electron microscopy image of mitochondria with cristae aligned in PBMCs (A). Effects of fasting and glucose load on percentage of mitochondria with aligned cristae (B). Representative transmission electron microscopy image of mitochondrial cristae after fasting and after glucose load in human PBMCs (C). Number of mitochondrial cristae per mitochondrial size (D) and total cristae length per mitochondrial size (E). Representative images of western blots (3 subjects) for the protein expression of MIC60, MIC19, and Ponceau (F). Effects of fasting and glucose load on MIC60 (G) and MIC19 (H) proteins. Proposed model created with BioRender.com (I). $n = 6$ healthy males, 4-6 cells per subject, >5 mitochondria per cell. In the graphs, each individual colored point represents an individual subject. The white arrows (A) show the aligned cristae. Glu, Glucose; Fast, Fasting

organelle interactions and the loss of their nutritional regulation can also be observed in *ob/ob* MNCs.

PBMCs have recently received increased interest for diagnostic purposes as their isolation from whole blood is relatively easy and minimally invasive. Moreover, they have gene expression patterns characteristic of certain diseases.[15,16] Interestingly, PBMCs are sensitive to nutritional challenges.[17,18,22] Indeed, it was shown in minipig that PBMCs metabolism acutely adapted to transition from fasting to feeding.[23] In humans, fasting induces increased gene expression related to fatty acid ß-oxidation in PBMCs,[17] as has been observed in peripheral tissues like liver and the skeletal muscle. Moreover, mechanisms of regulation into PBMCs seems similar to peripheral tissues, as PPARa is involved in fasting-induced regulation of gene expression in PBMCs.[17] However, our observations in PBMCs are exclusive for MetFlex, since we know that PBMCs are not always a good metabolic marker of skeletal muscle metabolic state, for example, in the exercise context.[24]

In this study, we found in PBMCs of two species (mice and humans) using two different techniques (in situ PLA and transmission electron microscopy) that the transition from fasting to fed state reduced mitochondria-ER interactions. This has previously been observed in murine liver.[8] This suggests that the adaptation of mitochondria-ER interaction to nutrient availability in PBMCs mirrors the adaptations in key metabolic tissues like the liver. In addition, we demonstrated in mice that alterations of mitochondria-ER interactions previously found in the liver[25]

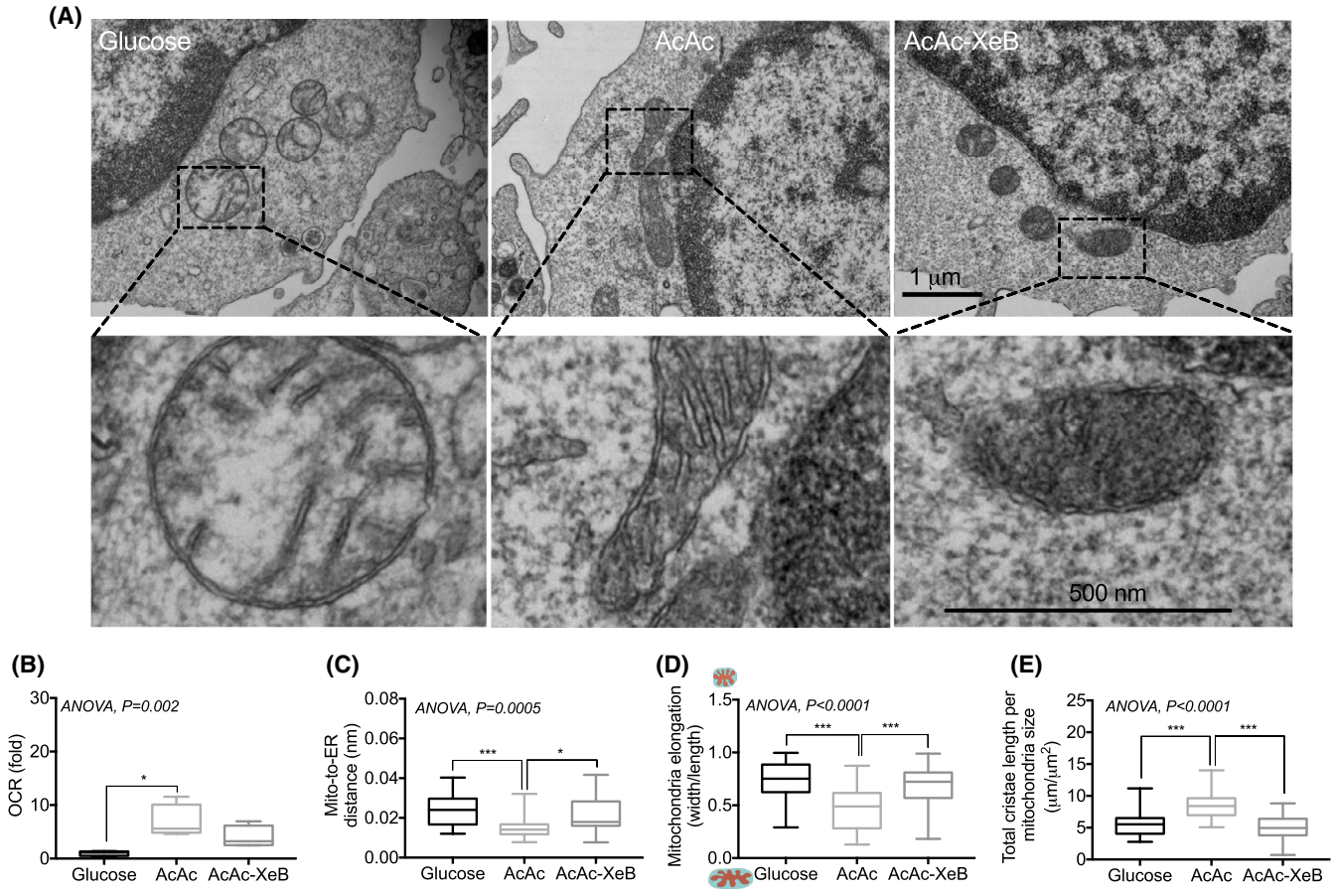

FIGURE 5 Effects of IP3R receptor activity on in vitro fasting substrate induce- mitochondrial-ER interaction, mitochondrial fusion phenotype and increases in mitochondrial cristae density in human PBMCs. Representative transmission electron microscopy image of PBMCs cultivated with glucose (10 mM), AcAc (10 mM) and AcAc (10 mM) + XeB (1 μM) for 4 hours (A). Effects of glucose, AcAc and AcAc+XeB on Basal OCR (B), mitochondria-ER distance (<50 nanometers) (C), mitochondrial network (D) and total cristae length per mitochondrial size (E) in human PBMCs. $n = 3$, >45 mitochondria per condition. AcAc, acetoacetate; XeB, xestospongin B

and skeletal muscle[26] of *ob/ob* mice were also present in *ob/ob* PBMCs, indicating that organelle miscommunication is a general alter in metabolic diseases. Together, these results suggest that mitochondria-ER interactions are a marker for cellular MetFlex.

Furthermore, our results show that the switch from the fasted to fed state is associated with reduced *OXPHOS* activity and mitochondrial fragmentation phenotype in human PBMCs. In accordance, we previously demonstrated in hepatocytes that glucose-mediated reduction of mitochondria-ER interaction is associated with decreased *OXPHOS* activity and mitochondria fission.[8] Additionally, previous in vivo and in vitro studies in skeletal muscle showed that: (a) fasting-fatty acid oxidation induced a mitochondrial fusion phenotype in murine skeletal muscle[27]; and (b) incubating murine muscle fibers with AcAc increased mitochondrial fusion and *OXPHOS* activity more than glucose stimulation.[28] With respect to above, two elegant studies using olimycin in combination with different substrates in MEFF cells and mouse skeletal muscle, demonstrated that *OXPHOS* activity regulates mitochondrial fusion. Therefore, we may speculate that the here observed greater calcium transfer from the reticulum to the mitochondria during fasting/AcAc observed, increased *OXPHOS* activity, and consequently, mitochondrial fusion.[28,29]

Previous studies have suggested that the alignment of mitochondrial cristae and mitochondrial cristae density are a dynamic process associated with *OXPHOS* activity.[30–32] Here, our results show that glucose consumption after fasting reduces mitochondrial cristae alignment, length and number, as well as reduces mitochondria-ER interaction, Mfn2 protein and CV-ATP5A levels. Once again, similar observations were previously made in the liver, as the postprandial state was associated with reduced mitochondria cristae length through a Mfn2 and Opa1-dependent mechanism.[11] Finally, we recently showed that a low Mfn2 protein abundance correlates with reduced mitochondria-SR interactions and mitochondrial cristae density in human skeletal muscle.[33] Our results indicate

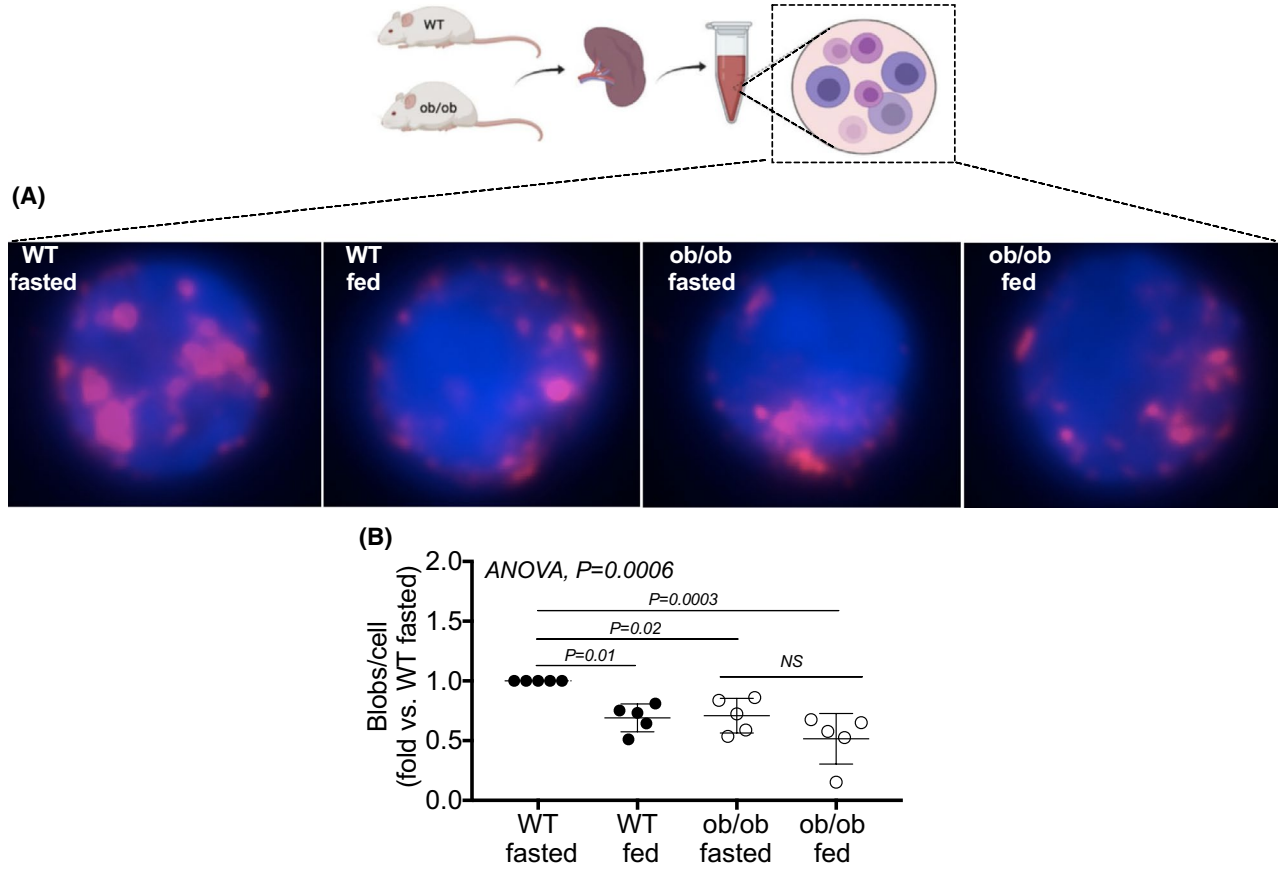

FIGURE 6 Mitochondria-ER interactions assessed through VDAC1/IP3R interactions using in situ proximity ligation assay (PLA) in spleen-derived mononuclear cells of wt and *ob/ob* mice after fasting and after feeding. Cartoon of mouse spleen-derived mononuclear cells (MNCs) isolation created with BioRender.com (A), and representative images and quantification of mitochondria-ER interactions measured by in situ PLA from murine spleen of wt and *ob/ob* mice after fasting and after feeding (B). $n > 15$ images per experiment, five independent series

that the fasting-feeding transition-induces mitochondrial dynamics modifications was not accompanied by changes in mitochondrial density as measured by Transmission electron microscopy and mitochondrial complexes density. The exception was the mitochondrial CV-ATP5A, which decreased after glucose load. However, mitochondrial CV-ATP5A seems to be indicator of the mitochondrial cristae density, rather than mitochondrial density[34,35]; therefore, the fasting-feeding transition-induces decrease in mitochondrial cristae density could potentially be explained by the decrease in mitochondrial CV-ATP5A. Finally, mitochondrial cristae dynamics are potentially regulated by nutritional cues in human PBMCs by Mfn2-regulated mitochondria-ER interaction and CV-ATP5A.

Cell physiology is largely controlled by cross-organelle communication. The interaction between the ER and mitochondria is one of the most studied interactions in which IP3R-mediated Ca^{2+} release plays a central role.[36] Ca^{2+} signals originating from IP3R activation regulate multiple cellular processes including apoptosis and autophagy.[37] Besides, ER-mitochondria Ca^{2+} exchange may regulate the mitochondrial dynamics response. For example, increased glucose availability reduces mitochondria-ER interaction and Ca^{2+} exchange in hepatocytes, and XeC treatment impairs glucose-induced mitochondrial dynamics.[8] Together, this suggests that acute glucose-induced mitochondrial adaptations depend on organelle Ca^{2+} exchange. Our results using in vitro challenged PBMCs are in accordance with previous hepatic observations, since XeB reduces mitochondria-ER Ca^{2+} exchange, and inhibits the effects of AcAc on the mitochondrial dynamics response. There are differences in the potency of xestospongins (A, B and C) to inhibit IP3R activity, it was previously demonstrated that XeC exhibited the highest IP3R activity blockage (7-fold higher potency compared to XeA); instead, the XeB, used in our study, displayed the lowest IP3R Ca^{2+} release inhibition, with a >16-fold decreased potency relative to XeC.[38] Therefore, slight inhibition of IP3R activity could affect cellular metabolism and potentially MetFlex. IP3R activity is modulated by Ca^{2+}, ATP, redox status, and various types of regulatory proteins, including kinases and phosphatases and certain oncogenes and tumor suppressors.[37,39]

In conclusion, mitochondrial dynamics responses (including mitochondrial network [mitochondrial fusion and fission], mitochondria-ER interaction and intramitochondrial dynamics to shape cristae and adjust matrix volume) acutely adapt to the metabolic transition from fasting to feeding in human PBMCs and reflect observations in murine peripheral tissues, such as the liver and skeletal muscle, in both healthy and pathological states. Therefore, our results suggest mitochondrial dynamics responses to be involved in MetFlex in humans. IP3R activity/ER-mitochondria Ca^{2+} exchange seems to be central to this and thus represents an interesting study topic in pathologies associated with low MetFlex in humans.

ACKNOWLEDGMENTS

The authors thank all the participants. This work was supported by the Unidad de Microscopía Avanzada UC (UMA UC) and Unidad de Microscopía Electrónica (UME) of the Universidad Austral de Chile.

DISCLOSURES

The authors declare no competing interests.

AUTHOR CONTRIBUTIONS

Mauricio Castro-Sepúlveda and Jennifer Rieusset conceived and designed research. Mauricio Castro-Sepúlveda, Béatrice Morio, Sebastian Jannas-Vela, Mauro Tuñón-Suárez, and Francisco Díaz-Castro performed experiments. Mauricio Castro-Sepúlveda, Béatrice Morio, Jennifer Rieusset, and Hermann Zbinden-Foncea analyzed data and interpreted results. Mauricio Castro-Sepúlveda, Béatrice Morio, and Jennifer Rieusset prepared figures. Mauricio Castro-Sepúlveda, Jennifer Rieusset and Hermann Zbinden-Foncea drafted manuscript; Mauricio Castro-Sepúlveda, Béatrice Morio, Sebastian Jannas-Vela, Mauro Tuñón-Suárez, Francisco Díaz-Castro, Jennifer Rieusset, and Hermann Zbinden-Foncea approved final version of manuscript. All authors wrote, revised, and approved the final version of the manuscript.

DATA AVAILABILITY STATEMENT

Contact the corresponding author for primary data material assessment.

ORCID

Béatrice Morio https://orcid.org/0000-0002-2418-1438
Mauro Tuñón-Suárez https://orcid.org/0000-0002-3085-9057
Francisco Díaz-Castro https://orcid.org/0000-0003-1644-8742
Jennifer Rieusset https://orcid.org/0000-0002-1587-2253
Hermann Zbinden-Foncea https://orcid.org/0000-0002-9643-1037

REFERENCES

1. Galgani JE, Moro C, Ravussin E. Metabolic flexibility and insulin resistance. *Am J Physiol Endocrinol Metab*. 2008;295(5):E1009-E1017.
2. Fernández-Verdejo R, Bajpeyi S, Ravussin E, Galgani JE. Metabolic flexibility to lipid availability during exercise is enhanced in individuals with high insulin sensitivity. *Am J Physiol Endocrinol Metab*. 2018;315(4):E715-E722.
3. Begaye B, Vinales KL, Hollstein T, et al. Impaired metabolic flexibility to high-fat overfeeding predicts future weight gain in healthy adults. *Diabetes*. 2020;69(2):181-192.
4. Fernández-Verdejo R, Castro-Sepulveda M, Gutiérrez-Pino J, et al. Direct relationship between metabolic flexibility measured during glucose clamp and prolonged fast in men. *Obesity (Silver Spring)*. 2020;28(6):1110-1116.
5. Gao AW, Cantó C, Houtkooper RH. Mitochondrial response to nutrient availability and its role in metabolic disease. *EMBO Mol Med*. 2014;6(5):580-589.
6. Eisner V, Picard M, Hajnóczky G. Mitochondrial dynamics in adaptive and maladaptive cellular stress responses. *Nat Cell Biol*. 2018;20(7):755-765.
7. Theurey P, Rieusset J. Mitochondria-associated membranes response to nutrient availability and role in metabolic diseases. *Trends Endocrinol Metab*. 2017;28(1):32-45.
8. Theurey P, Tubbs E, Vial G, et al. Mitochondria-associated endoplasmic reticulum membranes allow adaptation of mitochondrial metabolism to glucose availability in the liver. *J Mol Cell Biol*. 2016;8(2):129-143.
9. Castro-Sepulveda M, Jannas-Vela S, Fernández-Verdejo R, et al. Relative lipid oxidation associates directly with mitochondrial fusion phenotype and mitochondria-sarcoplasmic reticulum interactions in human skeletal muscle. *Am J Physiol Endocrinol Metab*. 2020;318(6):E848-E855.
10. Kondadi AK, Anand R, Reichert AS. Cristae membrane dynamics—a paradigm change. *Trends Cell Biol*. 2020;30(12):923-936.
11. Sood A, Jeyaraju DV, Prudent J, et al. A mitofusin-2-dependent inactivating cleavage of Opa1 links changes in mitochondria cristae and ER contacts in the postprandial liver. *Proc Natl Acad Sci U S A*. 2014;111(45):16017-16022.
12. Gottschalk B, Klec C, Waldeck-Weiermair M, Malli R, Graier WF. Intracellular Ca^{2+} release decelerates mitochondrial cristae dynamics within the junctions to the endoplasmic reticulum. *Pflugers Arch*. 2018;470(8):1193-1203.
13. Dlasková A, Engstová H, Špaček T, et al. 3D super-resolution microscopy reflects mitochondrial cristae alternations and mtDNA nucleoid size and distribution. *Biochim Biophys Acta Bioenerg*. 2018;1859(9):829-844.
14. Plecitá-Hlavatá L, Engstová H, Alán L, et al. Hypoxic HepG2 cell adaptation decreases ATP synthase dimers and ATP production in inflated cristae by mitofilin down-regulation concomitant to MICOS clustering. *FASEB J*. 2016;30(5):1941-1957.
15. Khan H, Anshu A, Prasad A, et al. Metabolic rewiring in response to biguanides is mediated by mROS/HIF-1a in malignant lymphocytes. *Cell Rep*. 2019;29(10):3009-3018.e4.
16. Senyilmaz-Tiebe D, Pfaff DH, Virtue S, et al. Dietary stearic acid regulates mitochondria in vivo in humans. *Nat Commun*. 2018;9(1):3129.
17. Bouwens M, Afman LA, Müller M. Fasting induces changes in peripheral blood mononuclear cell gene expression profiles

related to increases in fatty acid beta-oxidation: functional role of peroxisome proliferator activated receptor alpha in human peripheral blood mononuclear cells. *Am J Clin Nutr*. 2007;86(5):1515-1523.
18. Briet F, Twomey C, Jeejeebhoy KN. Relationship between metabolism and peripheral blood mononuclear cell mitochondrial complex I activity before and after a short-term refeeding in weight-losing cancer patients. *Clin Nutr*. 2003;22(3):247-253.
19. Bøyum A. Isolation of lymphocytes, granulocytes and macrophages. *Scand J Immunol*. 1976;5(Suppl):9-15.
20. Morabito C, Bosco G, Pilla R, et al. Effect of pre-breathing oxygen at different depth on oxidative status and calcium concentration in lymphocytes of scuba divers. *Acta Physiol (Oxf)*. 2011;202(1):69-78.
21. Del Campo A, Contreras-Hernández I, Castro-Sepúlveda M, et al. Muscle function decline and mitochondria changes in middle age precede sarcopenia in mice. *Aging (Albany NY)*. 2018;10(1):34-55.
22. de Mello VD, Kolehmanien M, Schwab U, Pulkkinen L, Uusitupa M. Gene expression of peripheral blood mononuclear cells as a tool in dietary intervention studies: what do we know so far? *Mol Nutr Food Res*. 2012;56(7):1160-1172.
23. Zeng Y, David J, Rémond D, Dardevet D, Savary-Auzeloux I, Polakof S. Peripheral blood mononuclear cell metabolism acutely adapted to postprandial transition and mainly reflected metabolic adipose tissue adaptations to a high-fat diet in minipigs. *Nutrients*. 2018;10(11):1816.
24. Rose S, Carvalho E, Diaz EC, et al. A comparative study of mitochondrial respiration in circulating blood cells and skeletal muscle fibers in women. *Am J Physiol Endocrinol Metab*. 2019;317(3):E503-E512.
25. Tubbs E, Theurey P, Vial G, et al. Mitochondria-associated endoplasmic reticulum membrane (MAM) integrity is required for insulin signaling and is implicated in hepatic insulin resistance. *Diabetes*. 2014;63(10):3279-3294.
26. Tubbs E, Chanon S, Robert M, et al. Disruption of mitochondria-associated endoplasmic reticulum membrane (MAM) integrity contributes to muscle insulin resistance in mice and humans. *Diabetes*. 2018;67(4):636-650.
27. Lee JY, Kapur M, Li M, et al. MFN1 deacetylation activates adaptive mitochondrial fusion and protects metabolically challenged mitochondria. *J Cell Sci*. 2014;127(Pt 22):4954-4963.
28. Mishra P, Varuzhanyan G, Pham AH, Chan DC. Mitochondrial dynamics is a distinguishing feature of skeletal muscle fiber types and regulates organellar compartmentalization. *Cell Metab*. 2015;22(6):1033-1044.
29. Mishra P, Carelli V, Manfredi G, Chan DC. Proteolytic cleavage of Opa1 stimulates mitochondrial inner membrane fusion and couples fusion to oxidative phosphorylation. *Cell Metab*. 2014;19(4):630-641.
30. Picard M, Gentil BJ, McManus MJ, et al. Acute exercise remodels mitochondrial membrane interactions in mouse skeletal muscle. *J Appl Physiol*. 2013;115(10):1562-1571.
31. Picard M, McManus MJ, Csordás G, et al. Trans-mitochondrial coordination of cristae at regulated membrane junctions. *Nat Commun*. 2015;6:6259.
32. Echeverria F, Jimenez Patino PA, Castro-Sepulveda M, et al. Microencapsulated pomegranate peel extract induces mitochondrial complex IV activity and prevents mitochondrial cristae alteration in brown adipose tissue in mice fed on a high-fat diet. *Br J Nutr*. 2021;126:825-836.
33. Castro-Sepulveda M, Fernández-Verdejo R, Tuñón-Suárez M, et al. Low abundance of Mfn2 protein correlates with reduced mitochondria-SR juxtaposition and mitochondrial cristae density in human men skeletal muscle: examining organelle measurements from TEM images. *FASEB J*. 2021;35(4):e21553.
34. De Los Rios Castillo D, Zarco-Zavala M, Olvera-Sanchez S, et al. Atypical cristae morphology of human syncytiotrophoblast mitochondria: role for complex V. *J Biol Chem*. 2011;286(27):23911-23919.
35. Salewskij K, et al. The spatio-temporal organization of mitochondrial F1FO ATP synthase in cristae depends on its activity mode. *Biochim Biophys Acta Bioenerg*. 2020;1861(1):148091.
36. Ahumada-Castro U, Bustos G, Silva-Pavez E, Puebla-Huerta A, Lovy A, Cárdenas C. In the right place at the right time: regulation of cell metabolism by IP3R-mediated inter-organelle Ca^{2+} fluxes. *Front Cell Dev Biol*. 2021;9:629522.
37. Roest G, La Rovere RM, Bultynck G, Parys JB. IP3 receptor properties and function at membrane contact sites. *Adv Exp Med Biol*. 2017;981:149-178.
38. Gambardella J, Morelli MB, Wang X, Castellanos V, Mone P, Santulli G. The discovery and development of IP3 receptor modulators: an update. *Expert Opin Drug Discov*. 2021;16(6):709-718.
39. Ivanova H, Vervliet T, Monaco G, et al. Bcl-2-protein family as modulators of IP3 receptors and other organellar Ca^{2+} channels. *Cold Spring Harb Perspect Biol*. 2020;12(4):a035089.

SUPPORTING INFORMATION

Additional supporting information may be found online in the Supporting Information section.

How to cite this article: Castro-Sepúlveda M, Morio B, Tuñón-Suárez M, et al. The fasting-feeding metabolic transition regulates mitochondrial dynamics. *FASEB J*. 2021;35:e21891. https://doi.org/10.1096/fj.202100929R